Electronic Supplementary Information for:

Et_3GeH versus Et_3SiH: Controlling Reaction Pathways in Catalytic C–F Bond Activations at a Nanoscopic Aluminum Chlorofluoride

G. Meißner,[a] D. Dirican,[a] C. Jäger,[b] T. Braun*[a] and E. Kemnitz*[a]

[a] Department of Chemistry, Humboldt-Universität zu Berlin, Brook-Taylor-Str. 2, 12489 Berlin, Germany

[b] Division 1, Bundesanstalt für Materialforschung und –prüfung, Richard-Willstätter-Str. 11, 12489 Berlin, Germany

1. Materials and Methods

The samples were prepared in a glovebox and the reactions performed in JYoung NMR tubes using conventional Schlenk techniques. C_6D_6 and C_6D_{12} were dried over K-Solvona® and distilled before usage. Et_3SiH was purchased from Sigma Aldrich and Et_3GeH form Alfa Aesar and were used as received and stored in glovebox. The liquid substrates 1-fluoropentane (Sigma Aldrich), 1-fluoroheptane (Sigma Aldrich) and 1-fluorohexane (Alfa Aesar) as well as the gaseous substrates fluoroethane, 1,1-difluroroethane and 1,1,1-trifluoroethane, purchased from abcr, were used as received. Aluminum chlorofluoride (ACF, $AlCl_xF_{3-x}$, x = 0.05-0.3) was synthesized according to the literature[1] on using anhydrous $AlCl_3$ (Sigma Aldrich) suspended in CCl_4, which was stored over molecular sieves, and CCl_3F (Fluka). NH_3-TPD measurements reveal that ACF contains roughly 1 mmol/g acidic sites.[2]

Liquid state NMR spectra (^1H, ^{19}F, $^{13}C\{^1H\}$) were acquired on a Bruker DPX 300, Bruker AVANCE II 300 or a Bruker AVANCE II 500 spectrometer at room temperature with tetramethylsilane as external standard. ^1H NMR chemical shifts (δ) were referenced to residual C_6D_5H (δ = 7.16 ppm) or $C_6D_{11}H$ (δ = 1.38 ppm) and $^{13}C\{^1H\}$ NMR spectra were referenced to the deuterated solvent (C_6D_6: δ = 128.1 ppm, C_6D_{12}: δ = 26.4 ppm). ^{19}F NMR spectra were calibrated externally to $CFCl_3$ (δ = 0 ppm) and $PhCF_3$ (δ = –63.7 ppm) was used as reference and external standard for quantification.

The ^1H and ^1H-^{29}Si cross-polarization (CP MAS) solid state NMR spectroscopic experiments were recorded on a Bruker AVANCE 600 spectrometer (B_0 = 14.1 T). All ^1H MAS NMR spectroscopic experiments were carried out at room temperature using a 2.5 mm magic angle sample spinning (MAS) probe. Data analysis was performed with the software TopSpin 2.1. The MAS frequency was 27.5 kHz for all ^1H MAS NMR spectroscopic experiments. The 90° pulse width was 2.8 μs and the EASY procedure (elimination of artifacts in NMR spectroscopy)[3] was used for the elimination of the strong ^1H probe background. 16 scans were accumulated and a repetition time of 20 s was used to avoid partial saturation. The ^1H chemical shift scale (δ) was referenced to tetramethylsilane using adamantane as secondary standard (δ = 1.78 ppm). The BaBa sequence[4] was used for the ^1H DQ (double quantum) measurements (Figure 1 in the main text). The DQ evolution time was set to 36.67 μs (one rotor period). 64 scans were accumulated for each t_1 increment. The t_1 increment was 73.73 μs (doubly rotor synchronized, i.e. two rotor cycles). The repetition time here was 5 s. ^1H-^{29}Si CP MAS experiments were carried out using a CP contact time of 2 ms, a MAS frequency of 9 kHz, a repetition time of 5 s, and 12000 scans were acquired. The ^{29}Si spin lock field was held constant while the ^1H spin lock field was ramped down to 50% of its initial value. ^1H TPPM decoupling was applied.[5] The ^{29}Si chemical shift is referenced with respect to TMS and calibrated to kaolinite as secondary standard (δ = –91.5 ppm).

The ^1H-^{13}C CP MAS, ^{29}Si MAS and ^{19}F Hahn spin-echo MAS NMR spectra were performed at room temperature using an AVANCE 400 spectrometer (B_0 = 9.4 T) equipped with a 4 mm probe head. All experiments were performed with a rotation frequency of 10 kHz. ^1H-^{13}C CP MAS NMR spectroscopic experiments were performed with a contact time of 1 ms, a recycle delay of 5 s and an accumulation number of 1635, i.e., a measurement time of about 2 h was sufficient to achieve a good signal to noise ratio. ^{13}C chemical shift values are given with respect to TMS and are measured against adamantane as secondary standard (δ = 29.5 ppm). The direct ^{29}Si MAS NMR spectrum was recorded with a 90° pulse width of 5 μs, a recycle delay of 60 s and using in total 10010 scans (7 days). The ^{29}Si chemical shift is referenced with respect to TMS and calibrated to Q_8M_8 (Octakis-(trimethylsiloxy)octasilsesquioxane) as secondary standard (δ = 11.5 ppm, low-field signal). ^{19}F MAS

NMR spectra were run with a 90° pulse duration of 2.4 μs, a spectrum width of 400 kHz, a recycle delay of 5 s and an accumulation number of 32. Rotor-synchronized Hahn spin-echo experiments were performed with the same parameters but an accumulation number of 512. One rotor period corresponds to a time of 100 μs. The isotropic chemical shifts δ_{iso} of ^{19}F resonances are given with respect to the $CFCl_3$ standard.

GC MS spectrometry was measured at an Agilent 6890N gas-phase chromatograph (Agilent 19091S-433 Hewlett-Packard) with an Agilent 5973 Network mass selective detector at 70 eV.

The experimental setup for performing a *Pulse*TA® (PTA) measurement[6] can be understood as an extension of usual TA MS devices by a gas dosing unit allowing for the injection of gases into the purge gas thus enabling an interaction with the solid. The measurements have to be prepared as usually in the case of simultaneously coupled TA MS investigations.[7] One obtains the thermoanalytical curves (DTA, TG) both under heating or isothermally whereby their interpretation is supported by additionally recorded ionic current (IC) curves in the multiple ion detection mode. For the present study, a NETZSCH thermoanalyzer STA 409 C *Skimmer*® system, equipped with a BALZERS QMG 421, was used.[7] Further experimental details are as follows: DTA TG sample carrier system; platinum crucibles (0.8 mL beaker); Pt/PtRh10 thermocouples; constant purge gas flow 70 mL/min Argon 5.0 (MesserGriesheim); isothermal temperature plateau; raw data evaluation with the manufacturer's software PROTEUS® (v. 4.3) and QUADSTAR® 422 (v. 6.02); no further data treatment. Samples of ca. 30 mg were measured versus empty reference crucible. Due to the sensitivity of ACF for humid air, the sample preparation had to respect several peculiarities such as filling and weighing of the crucible in a glove box and the transfer to the TA device in a tight plastic box. When setting the filled crucible onto the sample holder, a short access of humid air for approximately 60 s is unavoidable. Therefore, the ACF sample was subjected to a thermal pre-treatment in argon up to 150 °C prior to each PTA experiment. Substrates were injected either by using the commercially available PTA box or manually by using simple plastic syringes. Evaporable liquids can be pulsed as well by using a septum-tightened heated (120 °C) GC injector and ordinary μL glass syringes. Isothermal PTA revealed to be of extraordinary sensitivity for enthalpic effects and mass changes. The injection pulses as well as changes of the product composition of the gas phase are monitored by the IC curves of pre-chosen characteristic mass numbers for the injected agent and for presumed reaction products.

Synthesis of ACF · Et_3SiH and ACF · Et_3GeH: ACF (300 mg) was suspended in an excess of Et_3SiH (300 μL, 1.88 mmol) or Et_3GeH (300 μL, 1.85 mmol) in a Schenk flask. The reaction mixture was stirred at room temperature for 2 h. The excess of Et_3GeH or Et_3SiH was removed subsequently under reduced pressure. The resulting powders were stored in a glovebox and used for MAS NMR spectroscopic and PTA studies. For ACF · Et_3SiH, a weight increase by approximately 6% indicated a coverage of 55% of the Lewis acidic sites. The immobilization of Et_3GeH on ACF led to a weight increase of approximately 10%, suggesting a 62% coverage of the Lewis-acidic sites.

Isomerization of 1,2-dibromohexafluoropropane into 2,2,-dibromohexafluoropropane: This reaction can be used as an indication for the Lewis acidity of the catalysts, because only very strong Lewis acids show activity in this reaction at 25 °C.[8] ACF (25 mg), ACF · Et_3SiH (25 mg) or ACF · Et_3GeH (25 mg) were suspensed in 1,2-dibromohexafluoropropane (250 μL) and the reaction mixture was stirred for 2 h at 25 °C. After the reaction, $CDCl_3$ was added and the isomerization activity checked by

^{19}F NMR spectroscopy. In the case of ACF, the measurement revealed 100% conversion in constrast to the ACF · Et_3SiH and ACF · Et_3GeH with 0% of conversion.

2. MAS NMR Spectroscopic Studies of ACF · Et_3GeH

^{1}H MAS NMR (600.2 MHz): The spectrum shows next to resonances corresponding to the ethyl groups (δ = 1.1 ppm and δ = 1.6 ppm), two signals (δ = 3.8 ppm and δ = 4.2 ppm) in the range of signals for germane hydrogen (Figure S1, Figure 1 in the main text). Thus, the germane impregnation of ACF led to two types of surface bonded germane species.

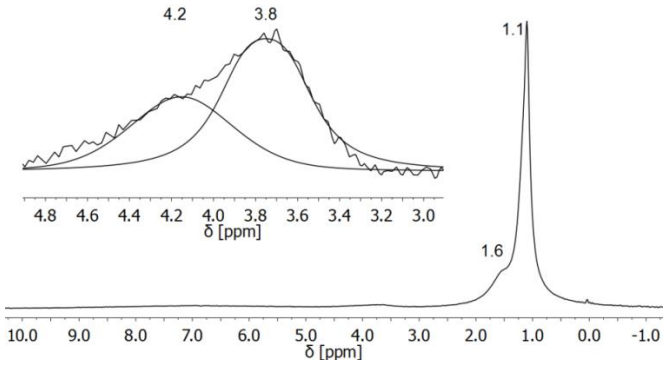

Fig. S1 ^{1}H MAS NMR spectrum of ACF · Et_3GeH with an enlarged region at about 4 ppm.

^{1}H-^{13}C CP MAS NMR (100.6 Mz): The two resonances (δ = 6.0 ppm and δ = 10.7 ppm) indicate the immobilization of Et_3GeH at the ACF surface (Figure S2). The chemical shifts are in accordance with the corresponding shifts of the ethyl groups of free Et_3GeH in C_6D_6 (δ = 3.8 ppm and δ = 10.3 ppm).

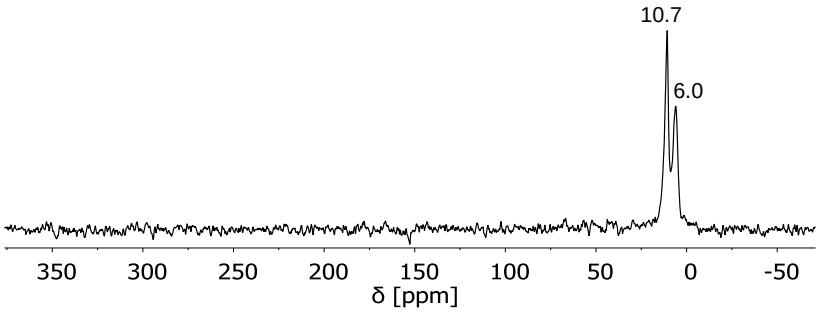

Fig. S2 ^{1}H-^{13}C CP MAS NMR spectrum of ACF · Et_3GeH.

^{19}F Hahn spin-echo MAS NMR: These pulse sequences are sensitive to homonuclear ^{19}F-^{19}F magnetic dipole-dipole couplings. Terminal or not well-incorporated fluorine atoms are detected due to the longer spin-spin relaxation times. In contrast, short spin-spin relaxation times T_2 of well bridged fluorine atoms show a decreased signal intensity after applying longer dipolar evolution times. A Hahn spin-echo MAS NMR spectroscopic experiment with 2 rotor periods (dipolar evolution time: 200 μs) is shown with suppression of the resonance corresponding to the bridged fluorine species (δ = –165 ppm and rotational side bands). The resulting NMR spectroscopic signal of the terminal fluoride species ($\delta \approx$ –200 ppm) can be detected (Figure S3). The terminal fluoride species are still present when ACF is treated with Et_3GeH, which is in contrast to the ^{19}F spin-echo MAS NMR spectra of ACF · Et_3SiH.[9]

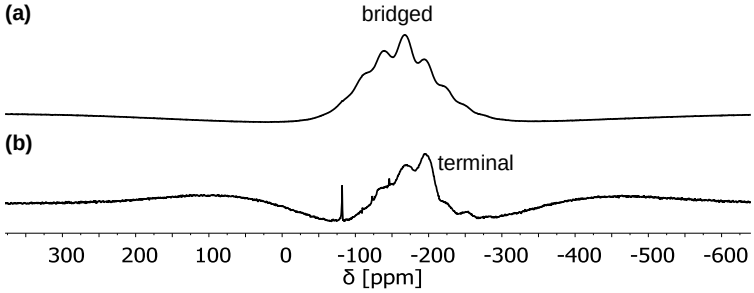

Fig. S3 Comparison of ^{19}F MAS NMR spectra of ACF · Et_3GeH indicating **(a)** bridged fluorine sites and **(b)** terminal fluorine sites using the ^{19}F rotor-synchronized Hahn spin-echo MAS NMR spectroscopic experiment; the intensity of the latter spectrum was enlarged by a factor of 16.

3. MAS NMR Spectroscopic Studies of ACF · Et_3SiH

^{1}H MAS NMR (600 MHz): The ^{1}H NMR MAS spectrum of ACF · Et_3SiH exhibits two signals at δ = 1.0 ppm and δ = 0.8 ppm for the ethyl groups of the silane and an apparently single resonance at δ = 3.8 ppm. The line fit, though, shows that this resonance possesses a very weak shoulder to the left (Figure S4). For comparison, the ^{1}H MAS NMR spectrum of ACF · Et_3GeH shows two resonances at δ = 3.8 ppm and δ = 4.2 ppm in the hydride area. These studies give information about different binding properties of the germane compared to the silane.

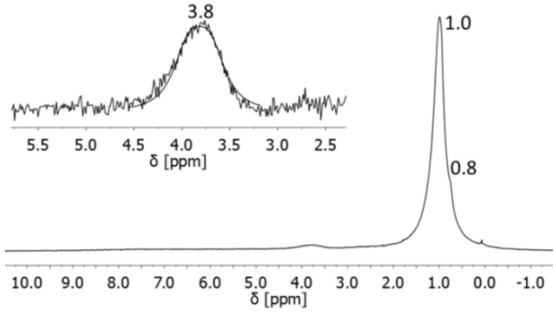

Fig. S4 ^{1}H MAS NMR spectrum of ACF · Et_3SiH with an enlarged region at about 4 ppm.

^{1}H-^{29}Si CP MAS NMR (119.2 MHz) and ^{29}Si MAS NMR (79.5 MHz): The ^{1}H-^{29}Si CP MAS NMR and the ^{29}Si MAS NMR spectra show a resonance at approximately δ = 75 ppm (Figure S5). The latter MAS NMR spectrum indicates the presence of only one silylium-like species at the surface, because there is no suppression of further signals which might occur applying cross polarization experiments. The chemical shift of ca. δ = 75 ppm is in a range for silylium cation-like species.[10]

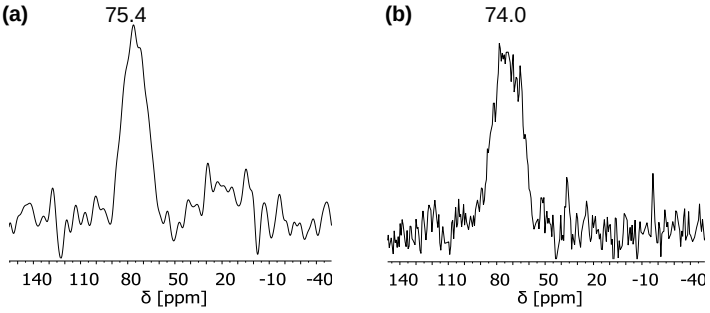

Fig. S5 Comparison of ^{29}Si MAS NMR spectroscopic experiments of ACF · Et_3SiH: **(a)** ^{1}H-^{29}Si CP MAS NMR spectrum and **(b)** ^{29}Si MAS NMR spectrum.

4. *Pulse*TA® Experiments

ACF with Et_3GeH: The isothermal (51 °C) PTA curves for the adsorption of Et_3GeH at ACF (25.2 mg) with the subsequent heating run is shown in Figure S6. Each pulse of Et_3GeH affects a mass gain of about 20 μg and an exothermal effect without exhibiting endothermal post-effects which would indicate a dissocoation of physisorbed Et_3GeH in the carrier gas flow. A mass increase of 230 μg was recorded leading to an immobilization of 0.48 mol-% (based on an estimated molar mass for ACF of 86.1 g/mol[11]). An exothermal interaction of ca. 0.8 μVs/mg between Et_3GeH and ACF is observed (Figure S6, left). The absence of any Et_3GeH desorption in the subsequent heating run proves a very strong interaction between ACF and Et_3GeH (Figure S6, right). Note that this interaction seems to be stronger than that of Et_3SiH on ACF due to a desorption at 100 °C and the exothermal interaction of 0.16 μVs/mg between Et_3SiH and ACF was monitored.[12]

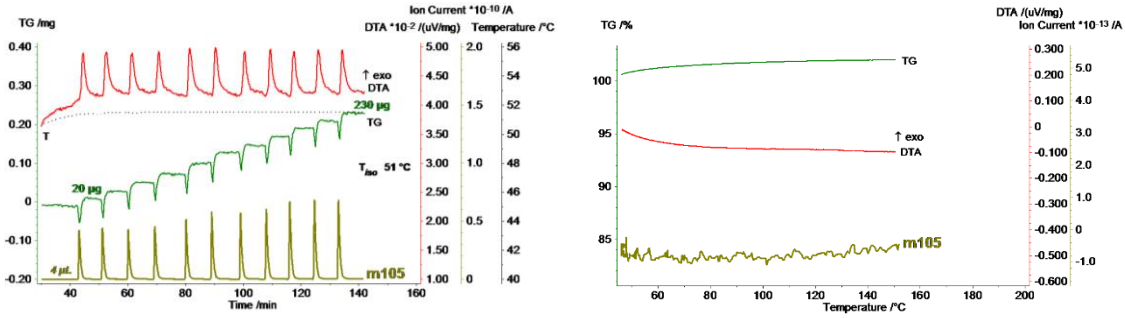

Fig. S6 Isothermal PTA curves of thermally pre-treated (140 °C) ACF (25.2 mg) in argon with the IC curve for the mass number m/z=105 ($EtGeH^+$) monitoring the sequence of 11 injection pulses of 4 μL Et_3GeH (25 μmol) (left) which did not saturate the ACF surface. Note that the DTA and the TG traces in the left plot indicate exclusively chemisorption; the sharp TG peaks downwards represent strong buoyancy effects due to the high density of the pulsed germane. The subsequent desorption experiment of the formed ACF · Et_3GeH did not reveal a liberation of Et_3GeH up to 160 °C (right).

ACF with 1-fluoropentane: The isothermal (31 °C) PTA curves for the adsorption of 1-fluoropentane at ACF (25.6 μg) with the subsequent heating run is shown in Figure S7. Each pulse of 1-fluoropentane affects a mass gain of ca. 10 μg and an exothermal effect without exhibiting endothermal post-effects which would indicate a dissocoation of physisorbed 1-fluoropentane in the carrier gas flow. A mass increase of 120 μg was recorded leading to an immobilization of 0.42 mol-% (based on an estimated molar mass for ACF of 86.1 g/mol[11]). An exothermal interaction of ca. 0.25 μVs/mg between 1-fluoropentane and ACF is observed (Figure S7, left). The absence of any 1-fluoropentane desorption in the subsequent heating run proves a veryfairly strong interaction between ACF and 1-fluoropentane (Figure S7, right).

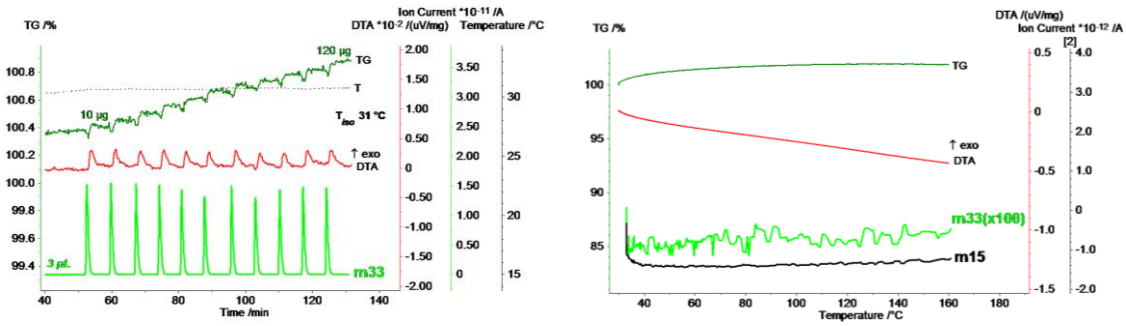

Fig. S7 Isothermal PTA curves of ACF (25.6 mg) in argon with the IC curve for the mass number m33 (CH_2F^+) monitoring the sequence of 11 injection pulses of 3 μL (26 μmol) 1-fluoropentane (left) which did not saturate the ACF surface. Note that the DTA and the TG traces in the left plot indicate exclusively chemisorption; the sharp TG peaks downwards represent strong buoyancy effects due to the high density of the pulsed 1-fluoropentane. The subsequent desorption experiment did neither reveal a liberation of 1-fluoropentane nor of organic fragments (m15) up to 160 °C (right). Note that the TG curve is not buoyancy-corrected as the messurement was started immediately after the loading step at 31 °C instead of the usual 25 °C.

5. General Procedure for Catalytic C–F Bond Activation of Liquid Substrates

Reaction parameters and results of the activation of 1-fluoropentane, 1-fluoroheptane and 1-fluorocyclohexane are summarized in Table S1. In a JYoung NMR tube, ACF · Et_3GeH or ACF · Et_3SiH was suspended in either Et_3GeH (1 equiv) or Et_3SiH (1 equiv) and C_6D_6 (0.6 mL). Then the substrate (1 equiv) was added. The reaction progress was monitored by ^1H and ^{19}F NMR spectroscopy. As a consequence of the Friedel-Crafts-type products using Et_3SiH as hydrogen source, the formation of H_2 next to HD was observed. The H_2 generation can be explained by the catalytic H/D exchange reactions with deuterated benzene at ACF.[2b] Conversions were calculated based on the consumed fluorinated substrate as well as of the hydrogen source to the corresponding products using a capillary with $PhCF_3$ ($\delta = -63.7$ ppm) as external standard. TONs were calculated based on the amount of fluorinated substrate assuming that 1 g of ACF contains roughly 1 mmol of catalytically active sites.[2]

Table S1 C–F bond activation reaction of primary fluoroalkanes at ACF

Entry	Hydrogen source	Substrate	$n_{substrate}$ [mmol]	$n_{act.\ sites}$[a]	Products	T [°C]	t [h]	Conv. [%][b]	TON[c]
1	Et_3GeH	fluoropentane	0.5	20	*E* / *Z*-2-pentene (3 : 1)	70	96	65	32
2[d]	Et_3GeH	fluoroheptane	0.5	20	*E* / *Z*-2-heptene (2 : 1), *E* / *Z*-3-heptene	70	72	84	21
3	Et_3GeH	fluorocyclohexane	1.5	15	cyclohexene[e]	70	96	75	75
4	Et_3SiH	fluoropentane	0.5	10	1-,2-,3-phenylpentane (1 : 8 : 2)	25	18	92	46
5[f]	Et_3SiH	fluoroheptane	0.5	10	1-,2-,3-phenylheptane	70	18	93	47
6[g]	Et_3SiH	fluorocyclohexane	1.5	10	Phenylcyclohexane, cyclohexene (1 : 1)	70	24	98	146

[a] The number of active sites on the ACF surface was calculated assuming 1 g of ACF contains roughly 1 mmol of catalytically active sites.[2] [b] Conversions were calculated using ^{19}F NMR spectroscopy based on the converted fluorinated substrate (1 equiv) and hydrogen source (1 equiv) into the corresponding products using $PhCF_3$ (capillary) as external standard. [c] TONs were calculated based on the amount of fluorinated substrate. [d] The integration of the signals of 3-heptene isomers was not possible, because no separated signal was found by $^1H,^{13}C$ HMQC NMR spectroscopy. [e] No additional hydroarylation[13] of cyclohexene into phenylcyclohexane was observed. The reaction of fluorocyclohexane (0.88 mmol) was faster ($n_{act.\ sites}$ = 5, 70 °C, 48 h) when it was run in Et_3GeH (0.88 mmol) and not in C_6D_6 yielding 100% conversion and TON = 176. [f] A determination of the isomer ratio was not possible, because no seperated signal was found by $^1H,^{13}C$ HMQC NMR spectroscopy. [g] Traces of cyclohexane were detected by ^{13}C NMR spectroscopy and hydroarylation[13] of cyclohexene into phenylcyclohexane was observed when the catalyst was not separated after the reaction.

After the reaction, the products were identified by characteristic signals using ^1H, $^{13}C\{^1H\}$, $^1H,^{13}C$ HMQC and ^{19}F NMR spectroscopy. Selected NMR resonances of reactants and products are summarized in Table S2 and Table S3. The isomer ratios were determined by integration of non-overlapping signals in the ^1H NMR spectra. The listed signals show no overlap with any other signals, which was also proofed by 2D $^1H,^{13}C$ HMQC NMR spectroscopy.

Table S2 Selected NMR resonances of reactants and products

Product	δ(^{1}H NMR) [ppm]	δ(^{13}C NMR) [ppm][a]
E-2-pentene	1.58 (m, 3H, H_3C–C=C)	133.4 (CH_3-C=**C**), 123.9 (CH_3-**C**=C), 26.1 (C=C-**C**H_2), 18.1 (CH_2**C**H_3), 14.2 (**C**H_3-C=C)
Z-2-pentene	1.51 (m, 3H, H_3C-C=C)	132.6 (CH_3-C=**C**), 123.3 (CH_3-**C**=C), 20.5 (C=C-**C**H_2), 14.3 (CH_2**C**H_3), 12.7 (**C**H_3-C=C)
E-2-heptene	1.60 (m, 3H, CH_3-C=C)	132.4, (CH_3-C=**C**), 124.8 (CH_3-**C**=C), 32.8 (C=C-**C**H_2), 32.2 (**C**-C-CH_3), 22.6 (**C**-CH_3), 18.1 (**C**H_3-C=C), 14.2 (C-**C**H_3)
Z-2-heptene	1.55 (d, 3H, CH_3-C=C)	131.1 (CH_3-C=**C**), 123.9 (CH_3-**C**=C), 32.2 (C=C-**C**H_2), 27.0 (**C**-C-CH_3), 22.7 (**C**-CH_3), 14.2 (C-**C**H_3), 12.9 (**C**H_3-C=C)
E-3-heptene	n.d.[b]	131.9 (CH_3-C-**C**=C), 129.3 (CH_3-C-C=**C**), 35.1 (**C**-C-CH_3), 26.0 (CH_3-**C**-C=C), 23.2 (C-**C**-CH_3), 14.3 (**C**H_3-C-C=C), 13.9 (C-C-**C**H_3)
Z-3-heptene	n.d.[b]	132.0 (CH_3-C-C=**C**), 129.3 (CH_3-C-**C**=C), 29.5 (**C**-C-CH_3), 23.3 (C-**C**-CH_3), 20.9 (CH_3-**C**-C=C), 14.4 (**C**H_3-C-C=C), 14.0 (C-C-**C**H_3)
Cyclohexene	5.64 (s, 2H, CH)	127.4 (C=C), 25.5 (C=C-**C**), 23.0 (C=C-C-**C**)
1-phenylpentane	2.48 (m, 2H, $C_{ar}CH_2$)	36.3 (Ph-C), 31.9 (Ph-C-**C**), 31.7 (Ph-C-C-**C**), 23.0 (**C**-CH_3), 14.2 (CH_3)
2-phenylpentane	2.55 (m, 1H, C_{ar}CH)	41.0 (Ph-C), 40.1 (Ph-C-**C**H_3), 22.6 (Ph-C-**C**H2), 21.2 (**C**-CH_3), 12.4 (CH_3)
3-phenylpentane	2.18 (m, 1H, C_{ar}CH)	50.0 (Ph-CH), 29.8 (CH_2), 12.4 (CH_3)
1-, 2-, 3-phenylheptane[c]	n.d.	n.d.
Phenylcyclohexane	2.38 (m, 1H, PhCH)	44.9 (Ph-C), 34.9 (Ph-C-**C**), 27.3 (Ph-C-C-**C**), 26.5 (Ph-C-C-C-**C**)
Cyclohexane	1.40 (s, 12H, CH_2)	27.2
H_2	4.48 (s)	–
HD	4.44 (t, $^{1}J_{H,D}$ = 42.0 Hz)	–

[a] NMR resonances of aromatic carbon atoms are not listed. [b] n.d. = not determined. [c] n.d. = not determined, the isomer identificatation was done by GC MS: 1-phenylheptane: *m/z* [M^{+}–C_6D_5]: 99; 2-phenylheptane: *m/z* (M^{+}–$C_8H_4D_5$): 71; 3-phenylheptane: *m/z* (M–$C_9H_6D_5$): 57.

Table S3 Selected NMR resonances of reactants and products

Reactant/product	δ(^{1}H NMR) [ppm]	δ(^{19}F NMR) [ppm]	δ(^{13}C NMR) [ppm]
Et_3GeH	1.06 (t, 9H, CH_3, $^{3}J_{H,H}$ = 7.8 Hz)	-	10.3 (s, CH_2), 3.8 (s, CH_3)
Et_3GeF	0.99 (t, 9H, CH_3, $^{3}J_{H,H}$ = 7.8 Hz)	-213.2 (m)	8.4 (d, CH_2, $^{2}J_{C,F}$ = 11.1 Hz), 7.4 (d, CH_3, $^{3}J_{C,F}$ = 1.9 Hz)
Et_3SiH	0.98 (t, 9H, CH_3, $^{3}J_{H,H}$ =7.9 Hz)	-	8.4 (s, CH_3) 2.8 (s, CH_2)
Et_3SiF	0.92 (t, 9H, CH_3, $^{3}J_{H,H}$ =8.0 Hz)	-176.5 (m)	6.3 (d, CH_3, $^{3}J_{C,F}$ =1.8 Hz) 5.2 (d, CH_2, $^{2}J_{C,F}$ =14.3 Hz)
Et_2SiF_2	0.80 (t, 6H, CH_3, $^{3}J_{H,H}$ =8.0 Hz)	-144.3 (m)	4.0 (t, CH_2, $^{2}J_{(C,F}$=15.0 Hz)
Fluoropentane	4.10 (dt, 2H, CH_2F $^{2}J_{H,F}$ = 47.6 Hz, $^{3}J_{H,H}$ = 6.2 Hz)	-219.0 (hept, $^{2}J_{F,H}$ = 24 Hz)	n.d.[a]
Fluoroheptane	4.12 (dt 2H, CH_2F $^{2}J_{H,F}$ = 47.5 Hz, $^{3}J_{H,H}$ = 6.1 Hz)	-219.0 (hept, $^{2}J_{F,H}$ = 24 Hz)	n.d.[a]
Fluorocyclohexane	4.32 (m, 1H, CHF)	-174.6 (m)	n.d.[a]

[a] n.d. = not determined.

The reaction of 1-fluoropentane with Et_3GeH (dehydofluoronation) and 1-fluoropentane with Et_3SiH (Friedel-Crafts-type reaction) and their reaction progress was monitored by NMR spectroscopy as shown in Figure S8 and S9.

1-Fluoropentane with ACF · Et_3GeH:

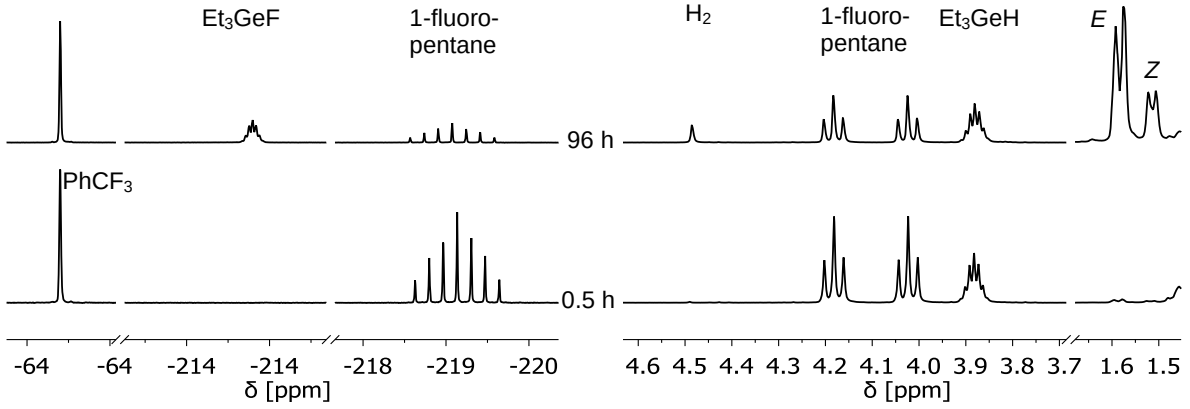

Fig. S8 Parts of the ^{19}F NMR (left) and ^{1}H NMR spectra (right) of the reaction progress for the dehydrofluorination reaction of 1-fluoropentane, $PhCF_3$ (δ = –63.7 ppm) was used as external standard. The ^{19}F NMR spectra shows the consumption of 1-fluoropentane with the generation of Et_3GeF. The corresponding ^{1}H NMR spectrum proves the conversion of 1-fluoropentane to *E*- and *Z*-2-pentene and H_2. Using C_6D_{12} as solvent gives the same results.

1-Fluoropentane with ACF · Et_3SiH:

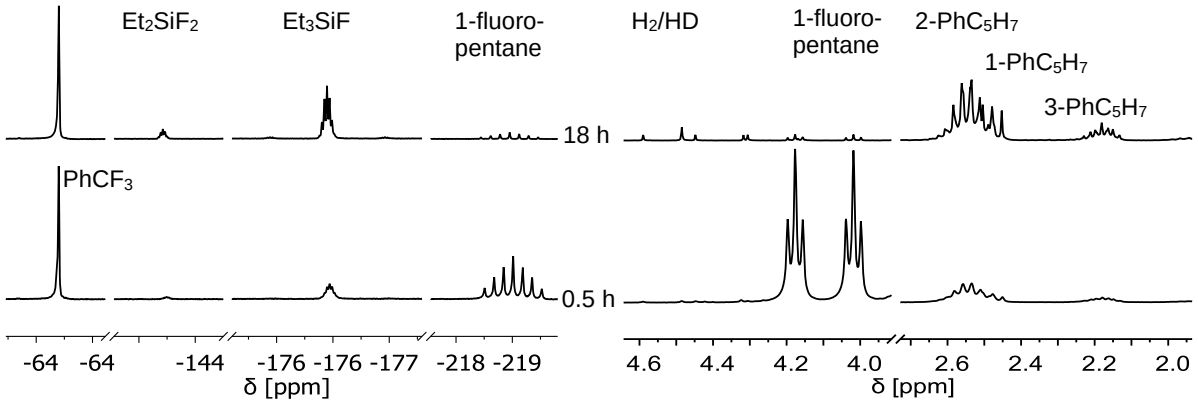

Fig. S9 Parts of the ^{19}F NMR (left) and ^{1}H NMR spectra (right) of the reaction progress for the Friedel-Crafts reaction of 1-fluoropentane, $PhCF_3$ (δ = –63.7 ppm) was used as external standard. The ^{19}F NMR spectra shows the consumption of 1-fluoropentane with the generation of Et_3SiF and Et_2SiF_2. The corresponding ^{1}H NMR spectrum proves the conversion of 1-fluoropentane to 1-phenylpentane, 2-phenylpentane and 3-phenylpentane, HD and H_2.

1-Fluoropentane with ACF and Et_3GeH or Et_3SiH: In a JYoung NMR tube, ACF was suspended in either Et_3GeH (0.33 mmol) or Et_3SiH (0.33 mmol) and C_6D_6 (0.6 mL). Then 1-fluoropentane (0.33 mmol) was added. The reaction progress was monitored at 70 °C for 4 days by ^{1}H and ^{19}F NMR spectroscopy. 1-Fluoropentane was consumed (100% conv., TON 13) and besides the products of dehydrofluorination and Friedel-Crafts-type reaction, Et_2GeF_2 (δ_{19F} = –168.5 (m) ppm) and Et_2SiF_2 (δ_{19F} = -144.3 (m) ppm) were formed as additional side products in a higher amount than starting with ACF · Et_3GeH or ACF · Et_3SiH as catalyst.

1-Fluoropentane and ACF: In a JYoung NMR tube filled with a PFA inliner, ACF (25 mg) was suspended in C_6D_6 (0.3 mL). Then 1-fluoropentane (0.33 mmol) was added. The reaction progress was monitored at 25 °C for 8 days by ^{19}F NMR spectroscopy. 1-Fluoropentane was consumed and DF ($\delta = -196.8$ ppm) was formed. The ^{1}H NMR spectrum showed the consumption of 1-fluoropentane and the formation of 1-phenylpentane, 2-phenylpentane and 3-phenylpentane. No full conversion was observed. To exclude the Friedel-Crafts type reaction, the same reaction parameters were used with C_6D_{12} (0.3 mL) as solvent, and the reaction was monitored by ^{1}H and ^{19}F NMR spectroscopy. Nearly no substrate was consumed and traces of 2-fluoropentane ($\delta = -174.8$ (m) ppm) and 3-fluoropentane ($\delta = -184.7$ (m) ppm) were identified by ^{19}F NMR spectroscopy, which were formed by HF addition to the double bond of 2-pentene. The corresponding reaction with ACF (25 mg) and Et_3SiH (0.33 mmol) in C_6D_{12} was not conclusive. Also when ACF · Et_3GeH (25 mg) was suspended in 1-fluoropentane (0.33 mmol) without additional Et_3GeH in C_6D_6 (0.6 mL), only small amounts of 2-pentene were formed until the immobilized Et_3GeH was consumed. The residual 1-fluoropentane was converted into the corresponding Friedel-Crafts products.

1-Fluoropentane with ACF and $^{n}Bu_3GeH$ or Ph_3GeH: In a JYoung NMR tube, ACF (25 mg) was suspended in $^{n}Bu_3GeH$ (0.33 mmol) or Ph_3GeH (0.33 mmol) was added. Then C_6D_6 (0.6 mL) and 1-fluoropentane (0.33 mmol) was added. The reaction progress was followed by ^{1}H and ^{19}F NMR spectroscopy and 1-fluoropentane was consumed. After 2 d at 70 °C a full conversion (TON = 12) to dehydrofluorination and Friedel-Crafts-products in a approximately ratio of 3 : 4 was observed with both hydrogen sources.

$AlCl_3$ as catalyst: In a JYoung NMR tube, $AlCl_3$ (25 mg) was suspended in either Et_3SiH (0.33 mmol) or Et_3GeH (0.33 mmol) and C_6D_6 (0.6 mL). Then 1-fluoropentane (0.33 mmol) was added. After adding the substrate to the reaction mixture, the reaction starts immediately, which in observed by gas evolution and an unidentified deposit was formed. The reaction progress was followed by ^{1}H and ^{19}F NMR spectroscopy and 1-fluoropentane was consumed. After 1 h at 25 °C a full conversion to 1-, 2- and 3-phenylpentane was observed with both hydrogen sources.

6. General Procedure for Catalytic C–F Bond Activation of Gaseous Substrates

Reaction parameters and results of the activation of 1-fluoroethane, 1,1-difluoroethane and 1,1,1-trifluoroethane are summarized in Table S4. In a JYoung NMR tube, ACF · Et_3GeH or ACF · Et_3SiH was suspended in either Et_3GeH (1 equiv) or Et_3SiH (1-3 equiv, depending on the number of C–F bonds at the substrate which can be activated) and C_6D_6 (0.6 mL). Then a defined volume of the substrate (1 equiv) was condensed into the reaction mixture from a small glass bulb filled with 1 atm of the gaseous substrate. Note, the dissolved amount of gaseous substrates is limited by their solubility in C_6D_6. The reaction progress was monitored by ^{1}H and ^{19}F NMR spectroscopy. As a consequence of the Friedel-Crafts-type products using Et_3SiH as hydrogen source, the formation of H_2 next to HD was observed. The H_2 generation can be explained by the catalytic H/D exchange reactions with deuterated benzene at ACF.[2b] Conversions were calculated based on the consumed fluorinated substrate as well as of the hydrogen source to the corresponding products using a capillary with $PhCF_3$ ($\delta = -63.7$ ppm) as external standard. TONs were calculated based on the amount of fluorinated substrate assuming that 1 g of ACF contains roughly 1 mmol of catalytically active sites.[2]

Table S4 C–F bond activation reaction of primary fluoroalkanes at ACF

Entry	Hydrogen source	Substrate	$n_{substrate}$ [mmol]	$n_{act.\ sites}$[a]	Products	T [°C]	t [h]	Conv. [%][b]	TON[c]
1[d]	Et_3GeH	CH_2FCH_3	0.54	15	ethene, phenylethane (1 : 2)	70	96	55	20
2[d]	Et_3GeH	CHF_2CH_3	0.68	25	vinyl fluoride, ethene, phenylethane (6 : 0.4 : 1)	70	120	11	3
3	Et_3GeH	CF_3CH_3	0.44	50	vinylidene fluoride	70	120	traces	–
4	Et_3SiH	CH_2FCH_3	0.54	15	phenylethane	70	24	100	36
5	Et_3SiH	CHF_2CH_3	0.68	15	phenylethane, 1,2-di-phenylethane (1.8 : 1)	70	18	100	91
6	Et_3SiH	CF_3CH_3	0.44	25	phenylethane, 1,2-di-phenylethane (1 : 1)	70	96	38	20

[a] The number of active sites on the ACF surface was calculated assuming 1 g of ACF contains roughly 1 mmol of catalytically active sites.[2] [b] Conversions were calculated by ^{19}F NMR spectra based on the converted fluorinated substrate (1 equiv) into the corresponding products using $PhCF_3$ (capillary) as external standard. [c] TONs were calculated based on the amount of fluorinated substrate. [d] The hydroarylation[13] of ethene into phenylethane can be observed when the catalyst is not separated after the reaction.

After the reaction, the products were identified by characteristic signals using ^1H, $^{13}C\{^1H\}$, $^1H,^{13}C$ HMQC and ^{19}F NMR spectroscopy. Selected NMR resonances of reactants and products are summarized in Table S5. The isomer ratios were determined by integration of non-overlapping signals in the ^1H NMR spectra The listed signals show no overlap with any other signals, which was also proofed by 2D $^1H,^{13}C$ HMQC NMR spectroscopy.

Table S5 Selected NMR resonances of reactants and products

Reactant/product	δ(^1H NMR) [ppm]	δ(^{19}F NMR) [ppm]	δ(^{13}C NMR) [ppm][a]
1-Fluoroethane	4.06 (dq, 2H, CH_2F, $^2J_{H,F}$ = 47.1 Hz, $^3J_{H,H}$ = 7.0 Hz)	-212.5 (m)	n.d.[b]
1,1-Difluoroethane	5.35 (dq, 2H, CHF_2, $^2J_{H,F}$ = 56.9 Hz, $^3J_{H,H}$ = 4.5 Hz)	-110.6 (dq, 2F, CHF_2, $^2J_{F,H}$ = 57 Hz, $^3J_{FH}$ = 21 Hz)	n.d.[b]
1,1,1-Trifluoroethane	1.16 (q, 3H, CH_3, $^3J_{H,F}$ = 12.9 Hz)	-62.0 (q, 3F, CF_3, $^3J_{F,H}$ = 13 Hz)	n.d.[b]
Ethene	5.26 (s, 4H, CH_2)	–	122.9 (CH_2)
Vinyl fluoride	6.26 (ddd, 2H, CHF, $^2J_{H,F}$ = 85.5 Hz, $^3J_{H,H}$ = 12.6 Hz, $^3J_{H,H}$ = 4.6 Hz)	-116.4 (ddd, 1F, CHF, $^2J_{FH}$ = 86 Hz, $^3J_{FH}$ = 54 Hz, $^3J_{FH}$ = 20 Hz)	154.4 (d, CHF, $^1J_{C,F}$ =260.6 Hz), 94.9 (d, CH_2, $^2J_{C,F}$ =8.5 Hz)
Vinylidene fluoride[c]	n.d.	-83.1	n.d.
Phenylethane	2.45 (q, 2H, CH_2, $^3J_{H,H}$ = 7.6 Hz) 1.09 (t, 3H, CH_3, $^3J_{H,H}$ = 7.6 Hz)	–	29.1 (CH_2) 15.9 (CH_3)
1,1-Diphenylethane	3.94 (q, 1H, CH, $^3J_{H,H}$ = 7.2 Hz), 1.46 (d, 3H, CH_3, $^3J_{H,H}$ = 7.2 Hz)	–	45.0 (CH) 22.1 (CH_3)

[a] NMR resonances of aromatic carbon atoms are not listed. [b] n.d. = not determined. [c] n.d. = not determined and recording a $^{19}F\{^1H\}$ NMR spectra showed the formation of traces.

1,1-Difluoroethane with ACF · Et_3GeH: The reaction progress of 1,1-difluoroethane with Et_3GeH (dehydofluoronation) was monitored by NMR spectroscopy as shown in Figure S10.

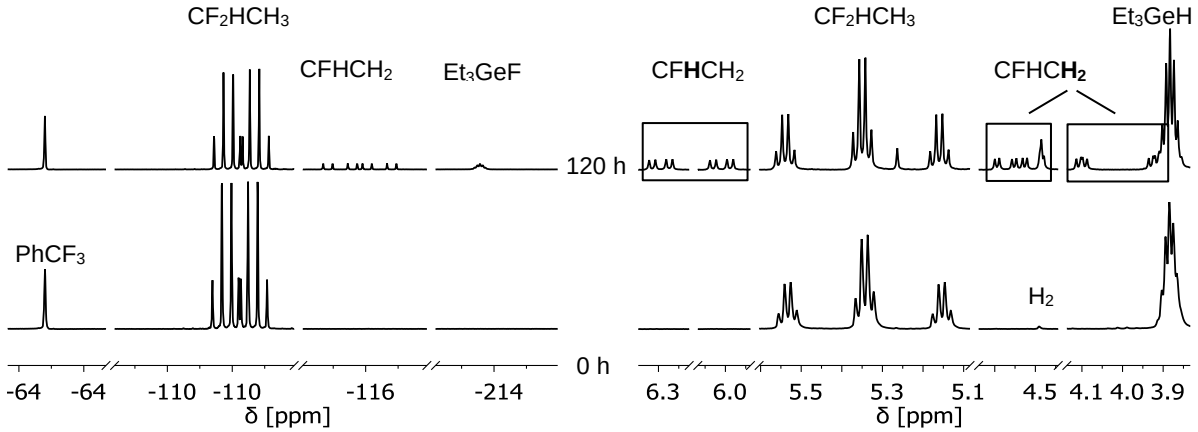

Fig. S10 Parts of the ^{19}F NMR (left) and ^{1}H NMR spectra (right) of the reaction progress for the dehydrofluorination reaction of 1,1-difluoroethane, $PhCF_3$ (δ = -63.7 ppm) was used as external standard. The ^{19}F NMR spectrum shows the consumption of 1,1-difluoroethane with the generation of vinyl fluoride and Et_3GeF. The corresponding ^{1}H NMR spectrum proves the conversion of 1-fluoropentane to vinyl fluoride and H_2.

6. Alternative Mechanism

As alternative to the silylium-/germylium supported mechanim (see main text), a C–F bond activation by ACF occurs first, followed by the generation of a carbenium-like species at the surface. Then the Friedel-Crafts products or olefins are formed and DF/HF generation is followed by a reaction with a silane or germane (Scheme S1).

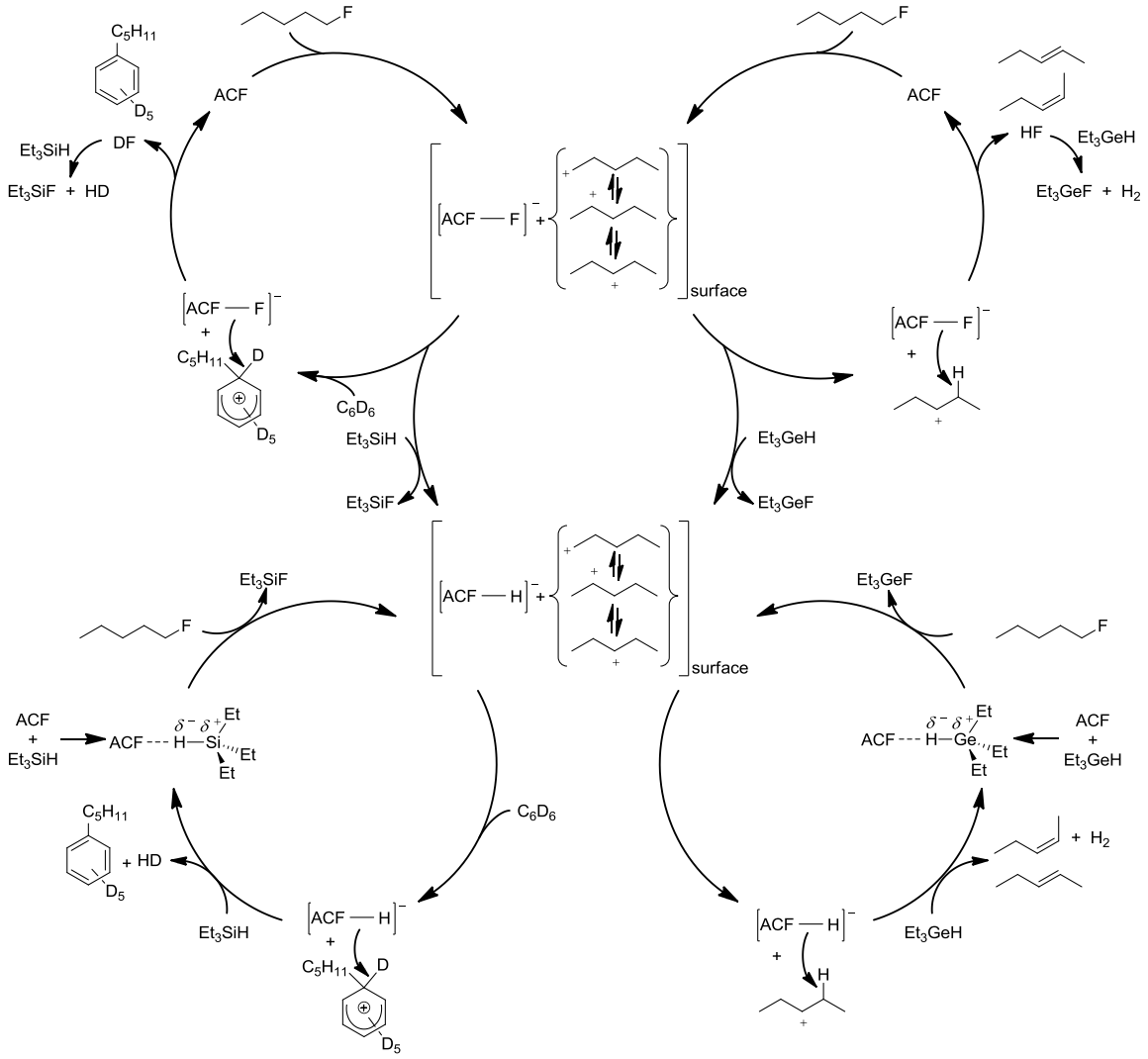

Scheme S1 Formation of a carbenium-like species at the surface of ACF as an alternative mechanism to the silylium/germylium supported mechanism.

7. References

1. (a) C. G. Krespan and V. A. Petrov, *Chem. Rev.*, 1996, **96**, 3269-3302, (b) T. Krahl, R. Stösser, E. Kemnitz, G. Scholz, M. Feist, G. Silly and J.-Y. Buzaré, *Inorg. Chem.*, 2003, **42**, 6474-6483.
2. (a) J. K. Murthy, U. Gross, S. Rüdiger, V. V. Rao, V. V. Kumar, A. Wander, C. L. Bailey, N. M. Harrison and E. Kemnitz, *J. Phys. Chem. B*, 2006, **110**, 8314-8319, (b) M. H. G. Prechtl, M. Teltewskoi, A. Dimitrov, E. Kemnitz and T. Braun, *Chem. Eur. J.*, 2011, **17**, 14385-14388.
3. C. Jaeger and F. Hemmann, *Solid State Nucl. Magn. Reson.*, 2014, **57–58**, 22-28.
4. M. Feike, D. E. Demco, R. Graf, J. Gottwald, S. Hafner and H. W. Spiess, *J. Magn. Reson., Ser A*, 1996, **122**, 214-221.
5. A. E. Bennett, C. M. Rienstra, M. Auger, K. V. Lakshmi and R. G. Griffin, *J. Chem. Phys.*, 1995, **103**, 6951-6958.
6. (a) M. Feist, *GIT Laborfachzeitschrift*, 2014, **58**, 31-34, (b) M. Feist, *ChemTexts*, 2015, **1**, 1-12.
7. E. Kaisersberger and E. Post, *Thermochim. Acta*, 1997, **295**, 73-93.
8. V. A. Petrov, C. G. Krespan and B. E. Smart, *J. Fluorine Chem.*, 1998, **89**, 125-130.
9. M. Ahrens, G. Scholz, T. Braun and E. Kemnitz, *Angew. Chem.*, 2013, **125**, 5436-5440 (*Angew. Chem. Int. Ed.*, 2013, **52**, 5328-5332).
10. (a) H. F. T. Klare and M. Oestreich, *Dalton Trans.*, 2010, **39**, 9176-9184, (b) M. Rohde, L. O. Müller, D. Himmel, H. Scherer and I. Krossing, *Chem. Eur. J.*, 2014, **20**, 1218-1222, (c) J. Chen and E. Y. X. Chen, *Angew. Chem.*, 2015, **127**, 6946-6950 (*Angew. Chem. Int. Ed.*, 2015, **54**, 6842-6846).
11. T. Krahl and E. Kemnitz, *J. Fluorine Chem.*, 2006, **127**, 663-678.
12. (a) M. Feist, M. Ahrens, A. Siwek, T. Braun and E. Kemnitz, *J. Therm. Anal. Calorim.*, 2015, **121**, 929-935, (b) A. Siwek, M. Feist, T. Braun and E. Kemnitz, *unpublished results*, 2016, (c) A. K. Siwek, M. Ahrens, M. Feist, T. Braun and E. Kemnitz, *ChemCatChem*, 2017, **9**, 839-845.
13. B. Calvo, J. Wuttke, T. Braun and E. Kemnitz, *ChemCatChem*, 2016, **8**, 1945-1950.